Pressurized carbon dioxide combined with aqueous ethanol as cosolvent induces efficient delipidation of porcine retina for their use as bioscaffolds

Alicia Gil-Ramírez*, Alice Spangenberg, Peter Spégel, Irene Rodriguez-Meizoso*

Lund University, Department of Chemistry, Centre for Analysis and Synthesis, P.O. Box 124, SE-22100, Lund, Sweden

*corresponding authors: aliciagilramirez@gmail.com, irenerome@gmail.com

Keywords: lipids; extracellular matrix; supercritical fluid chromatography; mass spectrometry

Declarations of interest: none

Abstract

Retina damage results in both health and social problems. To treat retina damage, extracellular matrix technology has gained interest in the scientist community. Bioscaffolds production is based in the use of a `cleaned` tissue, free of undesired cellular components, for further recellularization using healthy cells. Removal of lipids is an important step to improve both de- and recellularization. This work shows, for the first time, the efficiency of pressurized carbon dioxide (CO_2) fluids for the delipidation of porcine retina tissue. Pressurized CO_2-EtOH-H_2O (0.87 X_{CO2}) at 300 bar and 37 °C for 1h completely removed the 28 lipid species found in untreated retina (classified as phosphatidylcholines, phosphatidylethanolamines and sphingomyelins). When the ethanolic mixture was replaced by limonene at same conditions, lipid content decreased by more than a 50%, indicating reasonably good solubility of retina lipids in pressurized CO_2-limonene; however, no delipidation was observed using neat supercritical CO_2. In conclusion, pressurize CO_2 technologies can be applied for delipidation of retina. Whether the resulting bioscaffold can be recellularized and used in transplantation remain to be shown.

1. Introduction

According to the World Health Organization (WHO), 55 million people around the world restrict their normal life activities because of eye injuries [1]. It is estimated that around 1.6 million people are blind because of eye damage [1], which leads to elevated healthcare costs [2]. Most eye injuries, associated with retina damage, are attributed to such aspects of modern life as chronic stress, sedentary habits and excessive screen time. Retinal injuries can lead to an irreversible loss of vision by the release of cytokines and the subsequent stimulation of the immune system [3]. To date, medical advice that calls for lifestyle changes to minimize eye injuries has not been effective in encouraging behavioural change [2]. As a result, tissue regeneration has been explored as a feasible strategy for vision recovery.

The own-tissue regeneration approach involves the self-repairing of the tissues after injuries. Some human organs, e.g the liver, can regenerate when they are damaged however it is not applicable to the whole human body. To approach this challenge, regenerative medicine is mainly focused on the study of molecular signals that are capable of activating pluripotent stem cells when regeneration is needed. Unfortunately, there is not yet a clinically effective approach and, in this context, extracellular matrix (ECM) technology shows promise.

ECM technology is based on the generation of a platform (scaffold) with high similarity to the native ECMs and potentially invadable by healthy cells. Hydrogels, which are composed of hydrophilic crosslinked polymers , e.g. alginate or chitin, have been considered as leading candidates for ECM synthesis [4]. However, the mechanical properties of these structures are inferior to natural ECMs, their cellular penetration rates are low [4,5], and they need to be degraded completely *in-vivo*. These challenges could be managed by biomedical approaches based on decellularization of animal tissues. Removal of undesired cellular components from such tissues would generate biological scaffold materials (ECMs), which subsequently can be recellularized with healthy cells [6].

The undesirable cellular components include immune reactive structures such as proteins, DNA and lipids, which impair a proper recellularization. When properly decellularized, bio-ECMs can preserve some bioactive molecules from the native tissue such as glycosaminoglycans

or growth factors. These molecules, which are missing in the synthetic scaffolds, would positively influence the tissue acceptance by the recipient by promoting an enhanced recellularization process and a controlled immunoresponse [7–9].

At present, the most commonly used protocols for the decellularization of natural tissue and organs are based on the combination of physical, chemical and enzymatic methods [6]. Physical treatments, such as mechanical agitation or sonication, disrupt the cell membrane with a consequent release of intracellular components, which subsequently can be removed after rinsing of the tissue. Chemical-enzymatic protocols (usually detergents combined with DNases), aim to disrupt inter- and extra-cellular interactions for complete bio-ECM cleaning [6,10,11]. However, these treatments can negatively affect the biochemical composition, structure and mechanical properties of the scaffold. In addition, detergents residues could induce cytotoxicity during the recellularization process. Therefore, safer decellularization approaches are needed.

Pressurized carbon dioxide technology has been proposed as a nontoxic, non-residual and suitable one-step alternative to physical-chemical protocols for tissue decellularization [12–15]. It is believed that pressurized CO_2 fluids can solubilize lipids under certain conditions, determined mainly by the fluid composition (CO_2 with/without cosolvents) and parameters such as pressure and temperature [16]. How exactly the decellularization occurs is still unknown, although two potential explanations have been proposed: 1) the pressurized CO_2 fluid disrupts the cell first, as suggested for bacterial membrane [17], followed by a solubilization of cellular membrane lipids or 2) the bilayer membrane disruption occurs as a consequence of lipid desorption. Previous work has shown that the the extraction power displayed by pressurized CO_2 when combined with cosolvents, renders this technique a good candidate as a bio-ECM cleaner [13,18]. Pressurized CO_2 may lead to an efficient membrane disruption, facilitating later steps aiming at removing more polar components such as immune reactive DNA. Moreover, mechanical damages in the ECMs would be minimized due to the near-zero surface tension of supercritical carbon dioxide ($scCO_2$) [17].

Some authors have reported promising decellularization rates by pressurized CO_2 with or without cosolvents for heart valves, arteries, adipose tissue and bones [10–12,19,20]; however,

no studies have considered retina, which is a very mechanically sensitive tissue. Previous studies using pressurized CO_2 were usually performed at ~37 °C and up to 300 bar using ethanol as a cosolvent and found the absence of nuclei after treatment (denuclearization) to be the main effect. However, these results are limited in the absence of a delipidation analysis, which is relevant to determine the efficacy and selectivity of the decellularization fluid, especially when cosolvents are used. In addition, previous work has not tested whether the use of cosolvents other than ethanol might induce a high delipidation rates.

This work shows the efficiency of neat $scCO_2$, pressurized CO_2-EtOH-H_2O (95:5, v/v) and pressurized CO_2-limonene mixtures for delipidation of porcine retina tissues. Limonene was chosen as cosolvent because, while it contrasts with ethanol in terms of polarity, it is commonly used as defatting agent in industrial applications, which suggests that it is able to interact with lipid compounds. Lipids remaining in the treated tissue were identified and quantified by ultrahigh performance supercritical fluid chromatography (UHPSFC) coupled to quadrupole time-of-flight mass spectrometry (QTOF-MS/MS). We found that efficient delipidation can be achieved by submitting the retina tissues to pressurized CO_2-EtOH-H_2O (95:5, v/v). The results provide a foundation for novel biomedical application of pressurized CO_2 for retina transplant purposes.

2. Materials and Methods

2.1. Biological material

Porcine retinas (from Swedish landrace pigs and mini-pigs) were provided by the Department of Ophthalmology (Lund University, Sweden). All proceedings and animal treatment were in accordance with the guidelines and requirements of the government committee on animal experimentation at Lund University, the EU Directive 2010/63/EU for animal experiments, and with the ARVO statement on the use of animals in ophthalmic and vision research.

Retinas were cut into small pieces (6.25 mm^2 each) (Figure 1) and individually mounted on polycarbonate membranes in cell culture inserts (30 mm ⌀ and 0.4 μm pore size, Merck, Burlington, MA, USA) (Figure S1). Eight sections were dissected per eye (16 per individual)

(Figure 1). Following dissection, tissue sections were frozen and stored below -80 °C until further use.

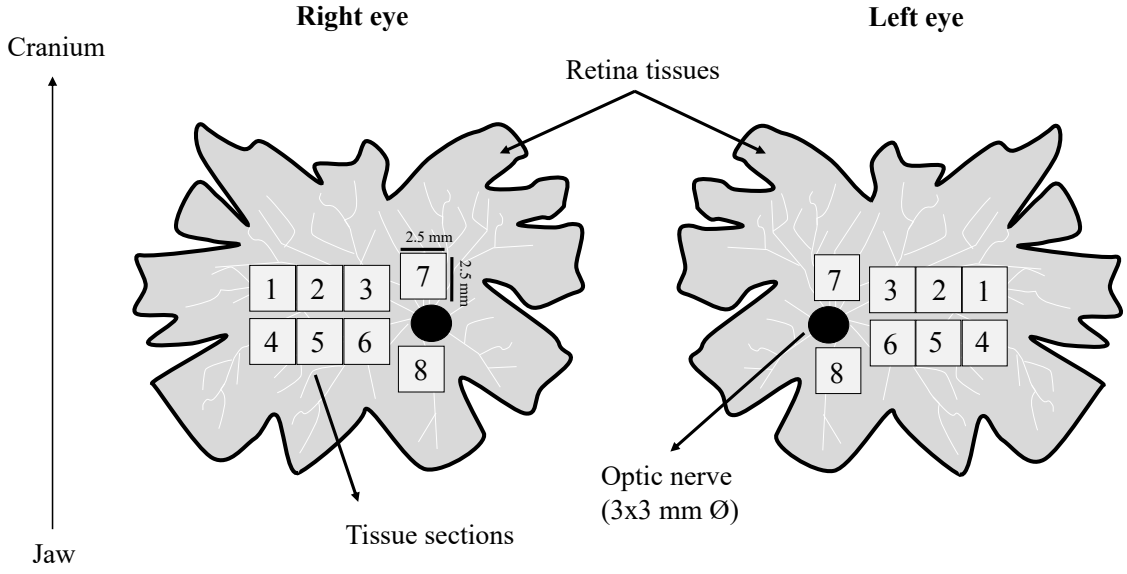

Figure 1. Representation of the retina tissue dissection. Samples were labelled using two digits. The first number corresponds to the eye: 1 and 2 denote the right eye and left eye, respectively, from the first individual; 3 and 4 the right eye and left eye, respectively, from the second individual; and so on. The second digit corresponds to the retina region sampled. For instance, the sample 4:3 corresponds to the region three of the retina from the left eye, individual two.

2.2. Reagents and standards

Ultrapure carbon dioxide (99.9993% purity) was provided by AGA GAS AB (Växjö, Sweden). Ethanol:water (95:5, v/v) and limonene (97% purity), used as cosolvents for the pressurized fluid treatment, were purchased from Solveco (Rosersberg, Sweden) and Sigma-Aldrich (St. Louis, MO, USA) respectively. Ultrapure water (18 Ω/cm) was produced by a Milli-Q devices from Merck Millipore (Darmstadt Germany).

For Folch extraction and lipid analysis, methanol (LC-MS grade) and dichloromethane (stabilized with about 0.002% of methyl-2-butene) were provided by VWR Chemicals (Fontenay-sous-bois, France). Ammonium formate (≥99% purity) was purchased from Sigma-Aldrich (St. Louis, MO, USA). Standard, 1,2-dipalmitoyl-sn-glycero-3-phosphocholine (DPPC; 16:0/16:0 PC ≥99% purity) and internal standard (IS), 1-pentadecanoyl-2-oleoyl(d7)-sn-glycero-3-

phosphocholine (15:0-18:1-d7-PC, 1mg/ml chloroform solution) were from Avanti Polar Lipids Inc. (Alabama, USA).

2.3. Pressurized carbon dioxide treatment

Polycarbonate membranes, containing the tissue sections, were placed on top of the sample container (Figure 2A). The sample container was specially constructed to provide an elevated fixed position inside the extraction vessel, thereby avoiding immersion of the tissue in the liquid cosolvent but allowing the free movement of the pressurized mixture of CO_2-cosolvent through the tissues.

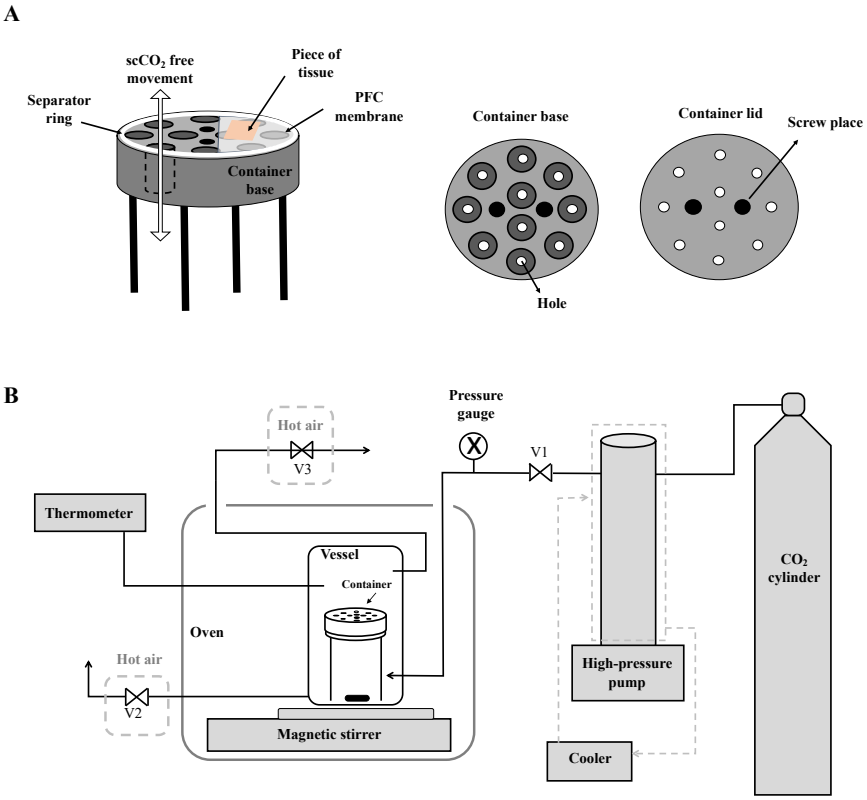

Figure 2. Details of the sample container (A) and scheme of the high-pressure system (B) used for tissue delipidation. V1-3 corresponds to needle valves. CO_2 in liquid state from a dip tube cylinder was pumped by a high-pressure pump. A thermometer was connected to the vessel for temperature monitoring during the process. Two connections were placed for the system depressurization, an upper one (controlled by V3) when neat CO_2 was used and the one in the bottom of the vessel (controlled by V2) for the depressurization when cosolvent was used.

The pressurized extraction equipment consisted in a home-built stainless-steel vessel of 80 ml volume (Ångström Laboratory, Uppsala University, Uppsala, Sweden), where the sample container is placed. The vessel was connected to a high-pressure syringe pump (Isco 260D, Teledyne Technologies Inc., NE, USA), which provided liquid CO_2 to the bottom of the device. To enable better control of the system, a pressure gauge was strategically placed between the needle valve (V1) and the pump. The vessel was equipped with two vent lines, the upper valve exclusively for CO_2 release and the lower one for cosolvent collection. The vessel was placed in a GC-oven (HP 5890 GC, Hewlett-Packard Co. CA, USA) and the temperature inside the vessel measured by a thermocouple. To facilitate solvent mixing, a magnetic stirrer (VWR, Leuven, Belgium) was used for the experiments with binary (limonene-CO_2) and tertiary (EtOH:H_2O (95:5, v/v)-CO_2) mixtures. A portable ventilation system was used for CO_2 release (Figure 2B).

For extractions including cosolvents, 15 mL of ethanol (95% pure ethanol, 5% water) or limonene were poured into the pre-heated extraction vessel (37 °C). Subsequently, the sample container was mounted and placed inside the extraction vessel before connecting the tubing. In order to avoid undesirable oxidation, the air inside the vessel was purged (V3, Figure 2B) and replaced by carbon dioxide. Then, the CO_2 charge was manually controlled to avoid drastic temperature increments. The pump was left running to maintain a constant pressure during the treatment to compensate for undetectable leaks, with averaged pump flows of 0.015 mL/min. Based on preliminary results from our group and the literature [21], the extraction of cell components was performed at 300 bar and 37 °C for 1h. These parameters were limited by the operational ranges of the equipment as well as by biological restrictions such as maximum physiological temperature (higher temperatures could lead to ECM degradation). The extraction time is based on that used for decellularization of cornea [19]. After treatment, the system was depressurized using the upper valve (V3, Figure 2B). For binary and tertiary mixtures, the cosolvent was collected using the lower valve (V2, Figure 2B) before depressurization. After depressurization, solvent remains were removed by a dynamic supercritical CO_2 (scCO2) rinse (85 bar, 37°C, 8 mL/min, one vessel volume). Treated retina tissues were kept at -80 °C until the analysis of remaining lipids.

2.4. Extraction of lipid residues from retina tissues

Prior to lipid extraction, retina tissues treated with pressurized fluids were re-hydrated with 50 µL of ultra-pure water to improve their removal from the polycarbonate membrane. Afterwards, tissues were dried overnight in a fridge at 5 °C and weighted. Fresh tissues were dried in parallel (control samples).

Lipid residues were extracted using two extraction methods described by Folch et al. (1957) [22] and Cífková et al. (2013) [23] and a method previously applied to porcine pulmonary arteries [24]. Time and shaking frequency were adapted for extraction of lipids from retina, with chloroform substituted for dichloromethane.

The efficiency of chloroform mixtures to extract lipids is well established however, CH_2Cl_2 has been shown to be a healthier and more secure solvent [25] and equally effective for total lipid extraction [25–27]. Moreover, the higher polarity of CH_2Cl_2 compared to $CHCl_3$ is known to facilitate extraction of more polar lipids [24].

Dried fresh and treated tissues were mixed with 600 µL of CH_2Cl_2:MeOH (2:1, v/v) and disrupted for 9 min (1 minute per cycle) at 15 Hz using a Qiagen TissueLyser (Qiagen GmbH, Hilden, Germany) in the presence of stainless steel beads. Subsequently, samples were vigorously shaken for 15 min at room temperature using a VX-2500 Multi-tube Vortexer (VWR, Fontenay-sous-Bois, France) and immediately centrifuged for 10 min at 10.000 rpm and 4 °C in a 5424R Eppendorf centrifuge (Hørsholm, Denmark). To induce phase separation by interfacial layer compression, 120 µL of 0.9% NaCl aqueous solution was added to the supernatant. Then, the mixture was shaken for 10 seconds at room temperature and centrifuged at 21 °C, 3000 rpm for 5 min. The lower phase was collected and dried under a flow of nitrogen (Reacti-Vap evaporating unit, Pierce). Extracts were weighed and kept at -80 °C until further analysis by UHPSFC/QTOF-MS/MS. Extraction blanks were produced using the same method, but with the tissue omitted.

2.5. Identification of lipids by UHPSFC-MS/MS

Dried untreated tissues (control samples, n=3) were used to identify lipid classes and species present in retina. The chromatographic separation of lipids was adapted from the method

reported by Gil-Ramirez, A et al. (2019)[24], in order to obtain complete separation of lipid classes being abundant in animal tissues i.e. triacylglycerols, glycerophospholipids, sphingolipids and sterol esters [23,28–31]. Lipid extracts were re-suspended in 50 µl of $CHCl_3$:MeOH (2:1, v/v) and analysed on an Acquity Ultra Performance Convergence Chromatography (UPC^2, Waters, MA, USA) with an Acquity UPC^2 Torus DIOL column (130Å, 1.7 µm, 3 mm x 100 mm, Waters, MA, USA) connected to a Torus DIOL (130Å, 1.7 µm, 2.1 mm x 5 mm, Waters, MA, USA) guard column. Column temperature was set at 50 °C and the back-pressure regulator at 110 bar. The injection volume was 1 µL and 10 mM ammonium formate in methanol was used as a modifier solvent. Lipids were eluted using a gradient: 0 min, 2%; 2 min, 2%; 4 min, 13%; 7 min, 27%; 8 min, 27%; 8.5 min, 2%; and 11 min, 2% modifier solvent, at a flow rate of 1.6 mL/min.

The Acquity UPC^2 equipment was coupled to a Xevo QTOF-MS (Waters, MA, USA) using a flow splitter (Acquity UPC^2 splitter, Waters, MA, USA). Two T-pieces (Waters, MA, USA) were used for backpressure control and an infusion of MeOH with 10 mM ammonium formate (0.25 mL/min) as makeup solvent. The mass spectrometer was operated in positive electrospray ionization mode, using a capillary voltage of 3.0 kV, a sampling cone voltage of 40 V, a source temperature of 120 °C, a drying temperature of 200 °C, a cone gas flow of 100 L/h and a drying gas flow of 800 L/h. Data were acquired in MS^E mode using a collision energy ramp of 15-45 eV with a scanning range of *m/z* 150−1000, and further processed using MassLynx v4.1 (Waters, MA, USA) and Mzmine2 [32].

Candidate lipids classes and lipid species from retina were identified by MS and MS/MS and data from LipidMaps® Lipidomics gateway (San Diego, CA) and published work [33]. The extraction efficiency was determined as the difference in signal-to-noise ratio (S/N) for treated and untreated tissue (n=3 each). Lipids were considered to be present in the sample when S/N for their monoisotopic mass was greater than 3.

2.6. Quantification of lipids by SFC-MS/MS

Lipids extracts were re-suspended in 50 µl of $CHCl_3$:MeOH (2:1, v/v) and spiked with the IS (5 µl) to a final IS concentration of 90 ppm. An external calibration curve was created for

PC16:0/16:0, the most abundant PC in retina, in $CHCl_3$:MeOH (2:1, v/v) from 0-300 ppm, with the IS at 90 ppm. PC16:0/16:0 was analysed by UHPSFC/QTOF-MS, as described above, and quantified as µg per mg dry tissue.

3. Results and discussion

3.1 Lipid classes identified in porcine retina

A similar lipid profile was individually found in all untreated samples from pigs and mini-pigs (n=3). The analytical method showed base-peak separation of lipid classes and within lipid class separation that depended on the acyl carbon number and the degree of saturation, as previously reported [24,34] (Figure 3).

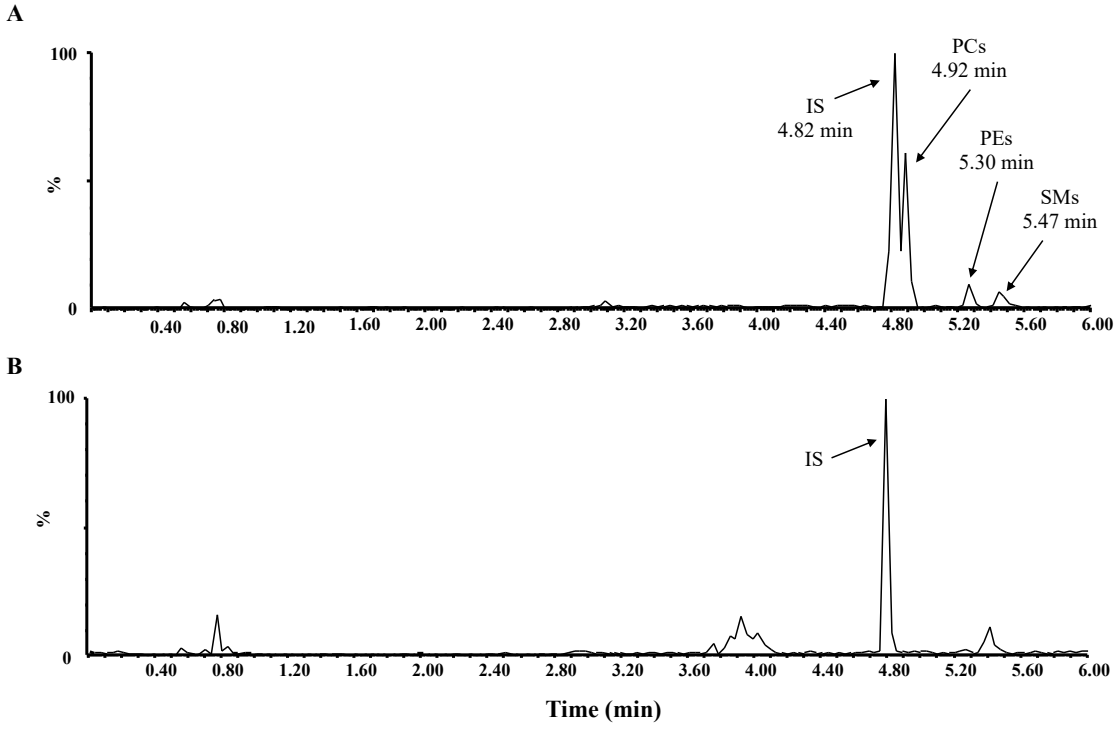

Figure 3. Example chromatogram of lipid extracts from untreated retina (A) and an extraction blank (B). The peak at 4.85 min corresponds to the IS. PCs were eluted first with retention times between 4.78 and 4.99 min, followed by PEs (5.16-5.34 min) and SMs (5.47-5.51 min).

In total, 28 lipid species ($[M+H]^+$) (Table 1), belonging to the classes of phosphatidylcholines (PCs), phosphatidylethanolamines (PEs) and sphingomyelins (SMs), were detected. These lipids

are among the most abundant polar lipids commonly found in biological tissues [23,28–31]. In line with this, previous studies have shown that about two-thirds of the lipids in retina tissues are phospholipids [35]. In our samples, the PCs were the most abundant species (57% of the total lipid species identified), followed by PEs and SMs (32 and 11% respectively).

Table 1. List of lipid species ($[M+H]^+$) found in porcine retina samples, ordered by retention time. IS, internal standard.

Retention time (min)	***m/z* experimental**	***m/z* calculated**	**Mass error (ppm)**	**Lipid I.D**
4.78	720.5926	720.5907	2.63	PC O-32:0
4.82	746.6068	746.6058	1.33	PC O-34:1; PC P36:1
4.82	762.6011	762.6008	0.39	PC 34:0
4.82	753.6162	753.6105	7.5	IS
4.85	734.5695	734.5695	0	PC 32:0
4.85	732.5565	732.5538	3.68	PC 32:1
4.85	786.6033	786.6008	-3.17	PC 36:2
4.85	760.5897	760.5851	6.04	PC 34:1
4.85	788.6169	788.6164	0.63	PC 36:1
4.88	784.5852	784.5851	0.12	PC 36:3
4.88	838.6354	838.6321	3.93	PC 40:4
4.88	810.5999	810.6008	-1.11	PC 38:4
4.88	782.5728	782.5695	4.21	PC 36:4
4.92	806.5717	806.5695	2.72	PC 38:6
4.92	834.6035	834.6008	3.23	PC 40:6
4.95	804.5598	804.5538	7.45	PC 38:7
4.99	830.5684	830.5695	-1.32	PC 40:8
5.16	746.5699	746.5694	0.66	PE 36:1
5.16	702.5419	702.5432	-1.85	PE O-34:2; PE P-34:1
5.23	768.553	768.5538	-1.04	PE 38:4
5.23	796.5854	796.5851	0.37	PE 40:4
5.26	750.5497	750.5432	8.66	PE O-38:6; PE P-38:5

5.26	776.5592	776.5589	0.38	PE O-40:7; PE P-40:6
5.26	740.5182	740.5225	-5.80	PE 36:4
5.3	792.553	792.5538	-1.00	PE 40:6
5.34	764.5233	764.5225	1.04	PE 38:6
5.47	787.6691	787.6687	0.50	SM 40:1
5.51	759.6398	759.6374	3.15	SM 38:1
5.51	731.6068	731.6061	0.95	SM 36:1

The identification of lipid classes was confirmed by their MS/MS spectra. PCs and SMs show an intense fragment at *m/z* 184.07 and PEs a characteristic neutral loss of 141 Da (Figure 4).

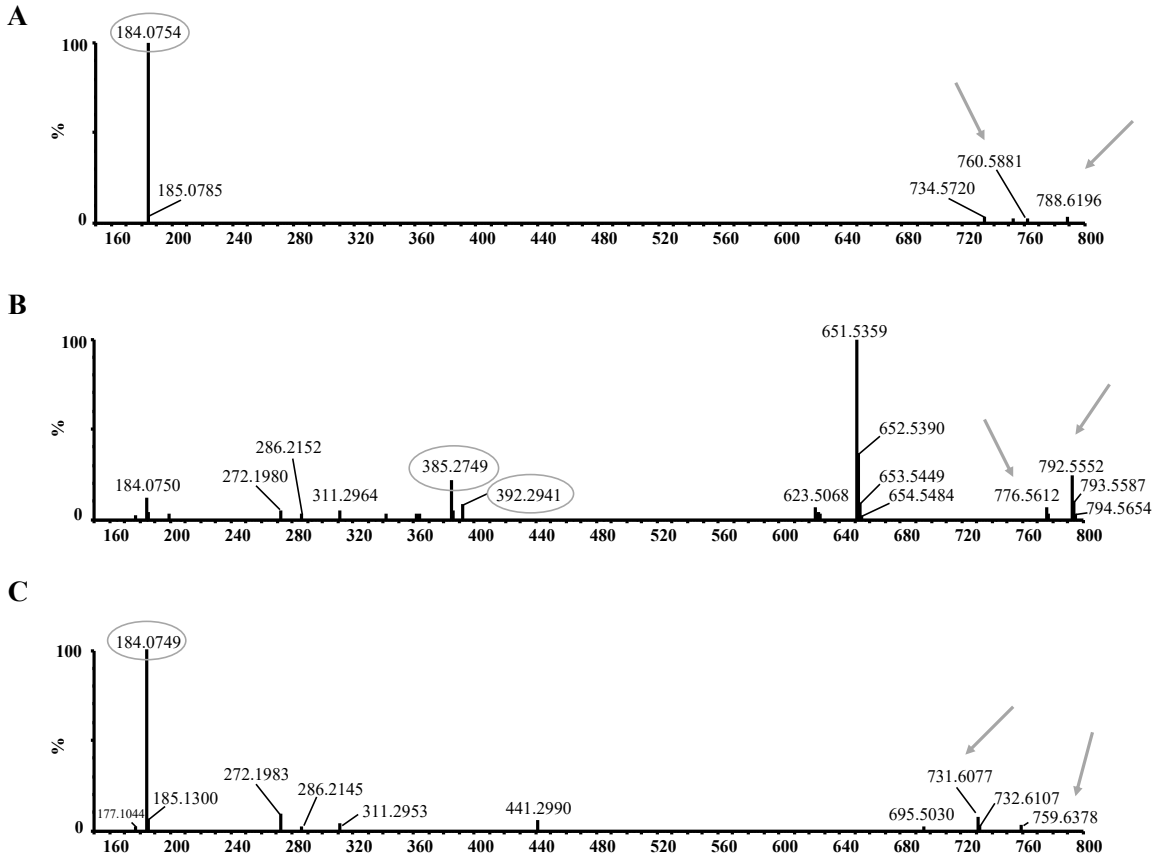

Figure 4. Example of the fragmentation pattern of the lipid class A) phosphocholines, B) phosphatidylethanolamines and C) sphingomyelins as obtained by MS/MS analysis. The arrows and circles indicate monoisotopic ions and characteristic fragments, respectively.

3.2. Exploring the biovariability of retina tissues

The removal of lipids from retina tissue by pressurized CO_2 might be influenced by the biovariability of porcine retina, which can hamper a coherent interpretation of the results. Biovariability may occur due to the combination of 1) inter-individual variability, and 2) a variable lipid distribution across retina regions [36][37]. Gravimetric analysis of lipid extracts from several individuals and tissue regions were used to study the lipid biovariability of porcine retina. Notable differences were found between three different eyes (from two individual), with lipid levels ranging from 86.33 to 368.42 µg per mg of tissue (Table 2). Moreover, a heterogeneous distribution of lipids along the same retina tissue could also contribute to the total biovariability. We found lipid levels to be higher further away from the optical nerve. Hence, lipid levels were higher in region 8, followed by regions 3 and 5 (Figure 1, Table 2). Our data supports previous findings of decreasing cell density with increasing distance to the optical nerve, a common cell distribution observed in retina from vertebrates animals [38].

Table 2. Gravimetric results of lipid content extracted from untreated tissues expressed as µg lipid extract per mg of dried sample.

Sample I.D	**Weight of dried tissue (mg) after extraction**	**Extracts containing lipids**	
		Weight of extract (µg)	**µg extract/ mg of dried tissue**
Eye 4 (indiv. N° 2)			
s4:3	0.41	50	122
Eye 1 (indiv. N° 1)			
s1:5	1.39	120	86
Eye 2 (indiv. N° 1)			
s2:8	0.38	140	368

To further investigate the biovariability, we performed an exhaustive quantification of the lipid content in the lipid extracts. Phosphatidylcholines, PC 32:0, PC 34:0, PC 34:1, PC 36:1,

PC 38:6 and PC 40:6, were selected as representatives for the most abundant lipid class in the tissue. The calibration curve was linear within 0-300 ppm of DPPC (R^2 of 0.99) (Figure S2). Sample 1:5 showed the lowest PC content with 8.9 µg PCs/mg dried tissue, followed by s4:3 and s2:8 with 42.0 and 130.6 µg PCs/mg dried tissue, respectively. Hence, these analyses confirmed a high variability (around 100% RSD) and were in agreement with the gravimetric analysis,
Since large variability was observed between eyes regardless of the individual, we inferred that lipid content was organ-dependent. In line with this, a deviation lower than 15% RSD in the lipid content per mg of dried tissue was observed in samples taken from the same eye (s4:4 and s4:5, individual 2, eye 4). Consequently, further analyses were performed by comparing treated and untreated samples from the same eye.

3.3 Delipidation of porcine retina tissue using pressurized CO_2-solvent mixtures

3.3.1. Investigation of the extraction fluid state

The physicochemcial properties of supercritical fluids are tuneable by parameters such as temperature, pressure and/or molar fractions of the fluid components, when cosolvents are used. However, the properties of a pressurized (not supercritical) mixture are different and possibly less affected by changes in pressure and temperature than the supercritical state. As these properties dictate the capacity of the fluid to extract target compounds, it is crucial to know the state of the fluid in the extraction process.

For example, a pressurized CO_2-EtOH mixture at 100 bar and 37°C with a CO_2 molar fraction of 0.99, will be in a supercritical state. However, if the CO_2 molar fraction drops below 0.96, then the mixture will no longer be supercritical, but rather defined as a pressurized fluid or pressurized solvent mixture (Figure S3).

All experiments were conducted at 300 bar and 37 °C. At these conditions, the fluid was in a supercritical state when neat CO_2 was used. The highest possible work pressure (300 bar) was selected to increase the pressurized CO_2-mixtures solvation power as much as possible while decreasing the selectivity [39], which would increase the possibility to remove a wider polarity

range of lipids from retina. However, presence of EtOH:H_2O (95:5, v/v) or limonene as cosolvents, resulted in a pressurized fluid. Addition of 15 mL cosolvent resulted in a CO_2 molar fraction of 0.87 for both EtOH:H_2O and limonene. A simulation of the phase diagram (GPEC 3.2.1, Phasety) showed that the fluid was near but not in supercritical state (Figure S3). A sapphire window, placed in the extraction vessel, allowed us to visually confirm that a one-phase system was achieved. These results are in agreement with previously published data [40]. A one-phase system prevents direct contact between the tissue and the liquid organic solvent, which would cause cytotoxic effects, and enhances diffusion of the otherwise liquid solvent into the solid sample. In the case of pressurized CO2 mixtures, the pressure was kept the same as for neat CO_2 for comparison, and because there is very little information in the literature about how solvation power of one-phase pressurized mixtures changes with pressure [41].

3.3.2. Determination of lipid residues in treated retina

Next, we determined residual lipids in retina tissues submitted to scCO_2, pressurized CO_2-EtOH-H_2O, and pressurized CO_2-limonene and compared with results from untreated tissue (Table 1). Tissue delipidation was quantified as the number of lipids with levels above a signal-to-noise-ratio of three [42], calculated for the area of the monoisotopic mass with the noise level determined from extraction blanks (Table 3).

Table 3. Signal-to-noise ratio (S/N) of the lipid species in treated samples. Values above 3 prove the presence of the respective lipid specie. Values between 3-10 indicate that lipid species were present in the samples but cannot be quantified.

Lipid specie	***m/z***	**S/N by fluid composition (CO_2 -)**					
		Neat (Eye 1:2)	**Neat (Eye 4:4)**	**Neat (Eye 4:5)**	**-EtOH-H_2O (Eye 4:1)**	**-EtOH-H_2O (Eye 4:2)**	**-limonene (Eye 2:7)**
PC O-32:0	720.5907	573.3	817.6	619.6	1.3	0.5	101.4
PC O-34:1; PC P36:1	746.6058	1742.6	1972.7	1769.7	0.8	0.4	589.7
PC 34:0	762.6008	2289.3	2603.8	2170.1	0.2	0.1	769.6
PC 32:0	734.5695	7706.1	9217.1	7923.8	2.3	0.2	3517.8

PC 32:1	732.5538	140.3	152.7	154.6	0.6	0.2	23.1
PC 36:2	786.6008	3004.4	3790.1	3164.7	1.5	0.2	705.4
PC 34:1	760.5851	745.4	825.8	729.1	0.1	0.0	324.7
PC 36:1	788.6164	1666.5	2010.5	1593.7	0.7	0.3	565.7
PC 36:3	784.5851	4824.4	5436.4	5486.2	1.5	0.9	2526.6
PC 40:4	838.6321	1939.0	2793.2	2243.7	4.3	1.0	538.7
PC 38:4	810.6008	15.9	19.4	22.5	0.1	0.0	0.1
PC 36:4	782.5695	5.4	11.7	3.9	0.4	0.1	0.7
PC 38:6	806.5695	14.6	32.2	23.1	0.5	0.2	2.2
PC 40:6	834.6008	962.9	1329.2	1251.3	0.1	0.1	225.9
PC 38:7	804.5538	8448.5	11453.5	10064.2	1.6	0.6	2648.4
PC 40:8	830.5695	1154.3	1524.2	1373.3	0.7	0.3	245.3
PE 36:1	746.5694	502.0	545.2	543.9	0.6	0.2	59.2
PE O-34:2; PE P-34:1	702.5432	263.2	284.6	231.0	0.9	0.3	59.4
PE 38:4	768.5538	458.0	503.9	378.8	1.4	0.5	96.1
PE 40:4	796.5851	46.6	44.3	30.7	1.0	0.3	10.4
PE O-38:6; PE P-38:5	750.5432	92.5	137.0	121.6	0.7	0.3	12.0
PE O-40:7; PE P-40:6	776.5589	1602.3	2051.2	1829.0	1.1	0.6	404.7
PE 36:4	740.5225	126.3	120.3	116.0	1.1	0.7	16.3
PE 40:6	792.5538	3.8	6.3	4.6	0.6	0.1	0.4
PE 38:6	764.5225	173.5	226.0	237.1	0.9	0.3	49.9
SM 40:1	787.6687	1658.7	1950.2	1440.8	9.6	3.7	250.3
SM 38:1	759.6374	57.1	85.7	56.4	0.5	0.1	6.7
SM 36:1	731.6091	1149.7	1573.3	1308.2	0.5	0.1	262.9

Pressurized CO_2-EtOH-H_2O was found to be the most efficient solvent mixture for lipid removal, with all lipids being undetected, except for SM 40:1 and PC 40:4 from eye 4:1 (Figure 5) (Table 3). The identified lipid classes, i.e. PCs, PEs and SMs, are among the most polar lipids found in biological tissues [23,28–31]. Extraction cannot only be discussed in terms of polarity of the solvent, but the efficient removal of these lipids using the EtOH-H_2O mixture is, most probably, greatly influenced by the hydrogen bonding capabilities of the solvent, contributing to a good solubility of these polar lipids.

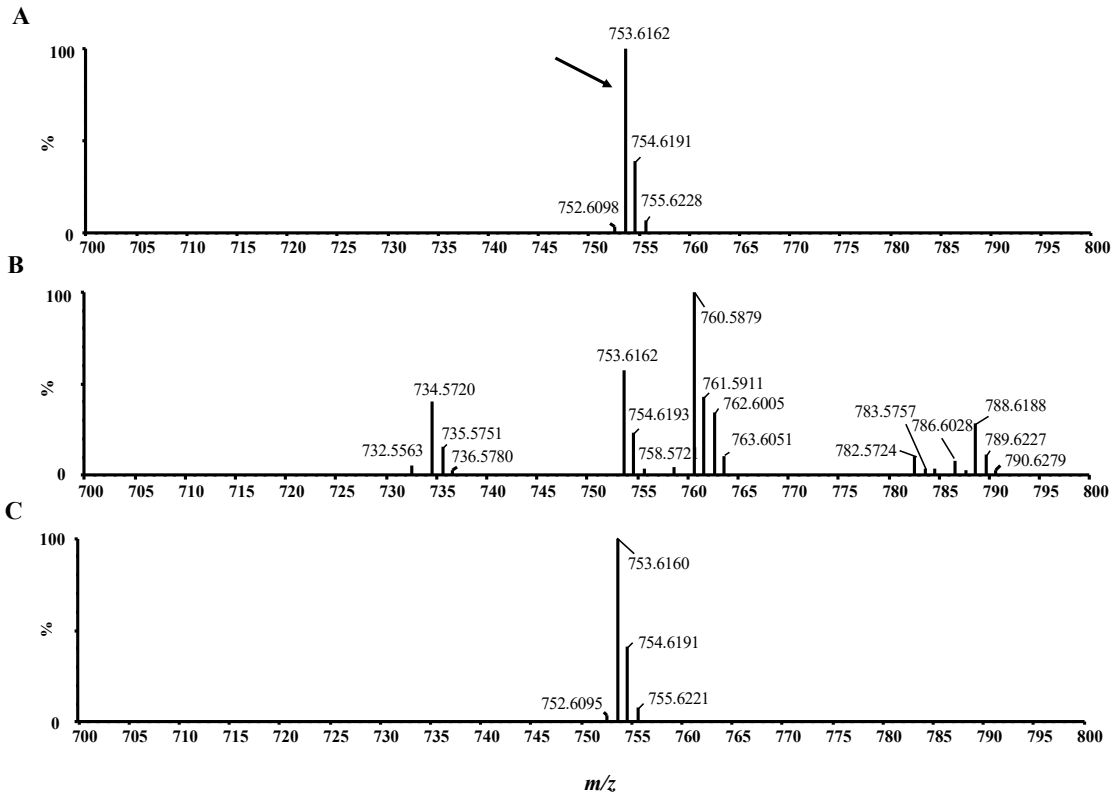

Figure 5. Representative mass spectra acquired at 4.85 min from analysis of A) retina treated with pressurized CO_2-EtOH-H_2O, B) fresh tissue and C) a spiked extraction blank. The arrow indicates the internal standard (IS) at *m/z* 753.616.

Neat $scCO_2$ treatment was less efficient in removing lipids from the tissue, as indicated by all detected lipids showing a S/N>3. This is true also for 38:4, PC 36:4, PC 38:6 and PE 40:6, which showed low S/N-ratios also in the untreated retina (Table S1). S/N-ratios for lipids from untreated and $scCO_2$ treated retina did not differ ($p>0.05$), suggesting an inefficient delipidation. Notably, a significant ionization suppression (Figure S4) was observed in the analysis of lipid extracts from neat $scCO_2$ ($p<0.01$) [43]. Hence, the S/N-ratios were likely underestimated for neat $scCO_2$.

The majority of lipid species, except for PC 38:4, PC 36:4, PC 38:6 and PE 40:6, from samples treated with pCO_2-limonene showed S/N >3 (Table 3). Untreated S/N *vs* treated S/N ratios (Table S1) were higher than one for all the lipid species, with the exception of PC 40:4 (Table S1). Hence, partial delipidation was achieved, but the process was much less efficient

when compared with pressurized CO_2-EtOH-H_2O. Consequently, we did not evaluate this solvent composition further. Regardless of the origin of the retina pieces, i.e. eye section or individual, repeatability was good considering the type of sample (16 and 23 %RSD for neat CO_2 and CO_2-EtOH-H_2O, respectively).

3.3.3. Quantification of residual lipids

Finally, the most abundant lipid species in untreated retina, PC 32:0, PC 34:0, PC 34:1, PC 36:1, PC 38:6 and PC 40:6, were quantified in untreated, neat scCO_2 and pressurized CO_2-limonene treated tissue from the same individual; lipids from pressurized CO_2-EtOH-H_2O treated retina were all below LOD. The selected PCs showed signals above their respective limits of quantification, except for PC 38:6 in samples treated with pressurized CO_2-limonene (Table 3). A partial delipidation was observed with CO_2-limonene, whereas neat scCO_2, was ineffective in extracting lipids from the tissue (Table S1). Levels of all detected PCs were reduced, and total detected PCs reduced by 66% (from 130.6 to 43.9 μg PCs/mg of dried tissue) after treatment with pressurized CO_2-limonene, as compared to the untreated sample (Figure 6A). Long-chain and saturated PCs were more efficiently removed, with PC 38:6 being undetected and PC40:6 being drastically reduced after treatment. Hence, PC 40:6, PC 34:0, PC 36:1, PC 32:0 and PC 34:1 were reduced by 71%, 65%, 61%, 59% and 57%, respectively. These results indicate a reasonably high solubility of retina lipids in pressurized CO_2-limonene, even though only dispersion forces are available for the interactions between the solvent and the lipids. Possibly, extraction may be driven by the formation of inverse micelles or liposomes from extracted lipids. Removal of retina lipids is nevertheless incomplete, suggesting that higher extraction times or solvent-to-sample ratios may lead to improved results. Regardless of the outcome of such experiments, the extraction efficiency for pressurized CO_2-limonene would in any case be lower than for pressurized CO_2-EtOH-H_2O since it would require longer times and larger amounts of solvent.

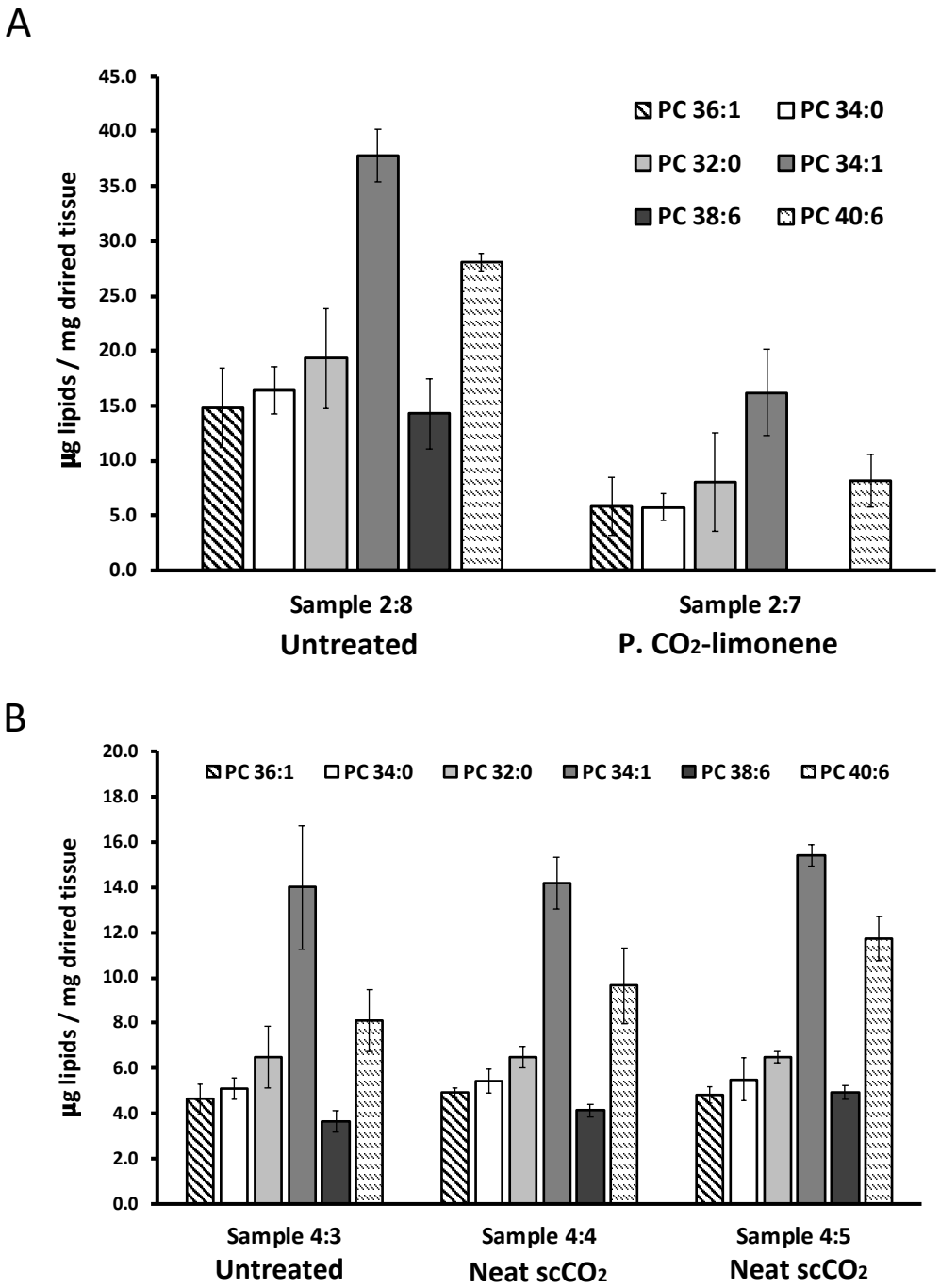

Figure 6. Residual lipids in retina tissue before and after treatment, expressed as µg of lipid class per mg of dried tissue, for (A) pressurized (P.) CO_2-limonene and (B) $scCO_2$ samples. Error bars show SE for n=3 SFC injections per sample.

Overall, our results show neat $scCO_2$ to be the least efficient solvent, among the tested solvent combinations, for extraction of lipids from retina. Undoubtedly, CO_2 is also the solvent

with the lowest polarity, which may hamper its ability to extract the polar lipid classes present in retina tissue.

4. Conclusion

The homebuilt device used for the lipid extraction by neat $scCO_2$ or pressurized CO_2-cosolvent was found to be suitable for the delipidation and to handle the recovery of retina tissue after treatment. Phosphatidylcholines, phosphatidylethanolamines and sphingomyelins, some of the most polar lipid classes present in biological tissue, were found exclusively in retina tissue by supercritical fluid chromatography coupled to quadrupole time of flight spectrometry. Lipid classes were satisfactorily separated within 6 minutes and 28 lipid species identified by the recognition of respective monoisotopic masses (MS) combined with their corresponding fragmentation patterns (MS/MS). We found pressurized CO_2-EtOH-H_2O to be superior to CO_2-limonene and neat $scCO_2$ for delipidation of retina tissue. Further studies are needed to evaluate the suitability of delipidated tissue as bioscaffolds.

Funding sources

This work has received funding from European Union´s Horizon 2020 research and innovation programme under the Marie Skłodowska-Curie Fellowship Grant Agreement No. H2020-MSCA-IF-2016-746137.

Acknowledgements

The authors would like to thank the Department of Ophthalmology at Lund University for supplying the retina tissue.

Declarations of interest

None

References

[1] A.-D. Négrel, B. Thylefors, The global impact of eye injuries, Ophthalmic Epidemiol. 5

(1998) 143–169. doi:10.1076/opep.5.3.143.8364.

[2] D. Pascolini, S.P. Mariotti, Global estimates of visual impairment: 2010, Br. J. Ophthalmol. 96 (2012) 614–618. doi:10.1136/bjophthalmol-2011-300539.

[3] T. Ren, Y. van der Merwe, M.B. Steketee, Developing Extracellular Matrix Technology to Treat Retinal or Optic Nerve Injury, ENeuro. 2 (2015). doi:10.1523/ENEURO.0077-15.2015.

[4] I.M. El-Sherbiny, M.H. Yacoub, Hydrogel scaffolds for tissue engineering: Progress and challenges, Glob. Cardiol. Sci. Pract. 2013 (2013) 316–342. doi:10.5339/gcsp.2013.38.

[5] H. Geckil, F. Xu, X. Zhang, S. Moon, U. Demirci, Engineering hydrogels as extracellular matrix mimics, Nanomedicine (Lond). 5 (2010) 469–484. doi:10.2217/nnm.10.12.

[6] T.W. Gilbert, T.L. Sellaro, S.F. Badylak, Decellularization of tissues and organs, Biomaterials. 27 (2006) 3675–3683. doi:https://doi.org/10.1016/j.biomaterials.2006.02.014.

[7] T.J. Keane, R. Londono, N.J. Turner, S.F. Badylak, Consequences of ineffective decellularization of biologic scaffolds on the host response, Biomaterials. 33 (2012) 1771–1781. doi:http://dx.doi.org/10.1016/j.biomaterials.2011.10.054.

[8] N. Turner, S. Badylak, Biologic scaffolds for musculotendinous tissue repair, Eur. Cell. Mater. 25 (2013) 130–143.

[9] P.M. Crapo, C.J. Medberry, J.E. Reing, S. Tottey, Y. van der Merwe, K.E. Jones, S.F. Badylak, Biologic scaffolds composed of central nervous system extracellular matrix, Biomaterials. 33 (2012) 3539–3547. doi:https://doi.org/10.1016/j.biomaterials.2012.01.044.

[10] L. Gui, A. Muto, S.A. Chan, C.K. Breuer, L.E. Niklason, Development of Decellularized Human Umbilical Arteries as Small-Diameter Vascular Grafts, Tissue Eng. Part A. 15 (2009) 2665–2676. doi:10.1089/ten.tea.2008.0526.

[11] A. Lichtenberg, I. Tudorache, S. Cebotari, S. Ringes-Lichtenberg, G. Sturz, K. Hoeffler, C. Hurscheler, G. Brandes, A. Hilfiker, A. Haverich, In vitro re-endothelialization of

detergent decellularized heart valves under simulated physiological dynamic conditions, Biomaterials. 27 (2006) 4221–4229. doi:10.1016/j.biomaterials.2006.03.047.

[12] J.K. Wang, B. Luo, V. Guneta, L. Li, S.E.M. Foo, Y. Dai, T.T.Y. Tan, N.S. Tan, C. Choong, M.T.C. Wong, Supercritical carbon dioxide extracted extracellular matrix material from adipose tissue, Mater. Sci. Eng. C. 75 (2017) 349–358. doi:http://dx.doi.org/10.1016/j.msec.2017.02.002.

[13] K. Sawada, D. Terada, T. Yamaoka, S. Kitamura, T. Fujisato, Cell removal with supercritical carbon dioxide for acellular artificial tissue, J. Chem. Technol. Biotechnol. 83 (2008) 943–949. doi:10.1002/jctb.1899.

[14] A. Zambon, M. Vetralla, L. Urbani, M.F. Pantano, G. Ferrentino, M. Pozzobon, N.M. Pugno, P. De Coppi, N. Elvassore, S. Spilimbergo, Dry acellular oesophageal matrix prepared by supercritical carbon dioxide, J. Supercrit. Fluids. 115 (2016) 33–41. doi:https://doi.org/10.1016/j.supflu.2016.04.003.

[15] J.L. Balestrini, A. Liu, A.L. Gard, J. Huie, K.M.S. Blatt, J. Schwan, L. Zhao, T.J. Broekelmann, R.P. Mecham, E.C. Wilcox, L.E. Niklason, Sterilization of Lung Matrices by Supercritical Carbon Dioxide, Tissue Eng. Part C. Methods. 22 (2016) 260–269. doi:10.1089/ten.TEC.2015.0449.

[16] F. Sahena, I.S.M. Zaidul, S. Jinap, A.A. Karim, K.A. Abbas, N.A.N. Norulaini, A.K.M. Omar, Application of supercritical CO2 in lipid extraction – A review, J. Food Eng. 95 (2009) 240–253. doi:https://doi.org/10.1016/j.jfoodeng.2009.06.026.

[17] G.C. Soares, D.A. Learmonth, M.C. Vallejo, S.P. Davila, P. González, R.A. Sousa, A.L. Oliveira, Supercritical CO2 technology: The next standard sterilization technique?, Mater. Sci. Eng. C. 99 (2019) 520–540. doi:https://doi.org/10.1016/j.msec.2019.01.121.

[18] D.M. Casali, R.M. Handleton, T. Shazly, M.A. Matthews, A novel supercritical CO2-based decellularization method for maintaining scaffold hydration and mechanical properties, J. Supercrit. Fluids. 131 (2018) 72–81. doi:https://doi.org/10.1016/j.supflu.2017.07.021.

[19] R.S. Hennessy, S. Jana, B.J. Tefft, M.R. Helder, M.D. Young, R.R. Hennessy, N.J.

Stoyles, A. Lerman, Supercritical Carbon Dioxide–Based Sterilization of Decellularized Heart Valves, JACC Basic to Transl. Sci. 2 (2017) 71–84. doi:https://doi.org/10.1016/j.jacbts.2016.08.009.

[20] J. Fages, A. Marty, C. Delga, J.S. Condoret, D. Combes, P. Frayssinet, Use of supercritical CO2 for bone delipidation, Biomaterials. 15 (1994) 650–656.

[21] Y.-H. Huang, F.-W. Tseng, W.-H. Chang, I.-C. Peng, D.-J. Hsieh, S.-W. Wu, M.-L. Yeh, Preparation of acellular scaffold for corneal tissue engineering by supercritical carbon dioxide extraction technology, Acta Biomater. 58 (2017) 238–243. doi:https://doi.org/10.1016/j.actbio.2017.05.060.

[22] J. Folch, M. Lees, G.H.S. Stanley, A SIMPLE METHOD FOR THE ISOLATION AND PURIFICATION OF TOTAL LIPIDES FROM ANIMAL TISSUES, J. Biol. Chem. 226 (1957) 497–509. http://www.jbc.org/content/226/1/497.short.

[23] E. Cífková, M. Holčapek, M. Lísa, Nontargeted Lipidomic Characterization of Porcine Organs Using Hydrophilic Interaction Liquid Chromatography and Off-Line Two-Dimensional Liquid Chromatography–Electrospray Ionization Mass Spectrometry, Lipids. 48 (2013) 915–928. doi:10.1007/s11745-013-3820-4.

[24] A. Gil-Ramírez, S. Al Hamimi, O. Roskmark, O. Hallgren, A.-K. Larsson-Callerfelt, I. Rodríguez-Maizoso, Efficient methodology for the extraction and analysis of lipids from porcine pulmonary artery by supercritical fluid chromatography coupled to mass spectrometry, J. Chromatogr. A. (2019). doi:10.1016/j.chroma.2019.01.064.

[25] E. Cífková, M. Holčapek, M. Lísa, M. Ovčačíková, A. Lyčka, F. Lynen, P. Sandra, Nontargeted Quantitation of Lipid Classes Using Hydrophilic Interaction Liquid Chromatography–Electrospray Ionization Mass Spectrometry with Single Internal Standard and Response Factor Approach, Anal. Chem. 84 (2012) 10064–10070. doi:10.1021/ac3024476.

[26] K. Sterz, G. Scherer, J. Ecker, A simple and robust UPLC-SRM/MS method to quantify urinary eicosanoids, J. Lipid Res. 53 (2012) 1026–1036. doi:10.1194/jlr.D023739.

[27] O.L. Knittelfelder, B.P. Weberhofer, T.O. Eichmann, S.D. Kohlwein, G.N. Rechberger,

A versatile ultra-high performance LC-MS method for lipid profiling, J. Chromatogr. B. 951–952 (2014) 119–128. doi:https://doi.org/10.1016/j.jchromb.2014.01.011.

[28] S.K. Abbott, A.M. Jenner, T.W. Mitchell, S.H.J. Brown, G.M. Halliday, B. Garner, An Improved High-Throughput Lipid Extraction Method for the Analysis of Human Brain Lipids, Lipids. 48 (2013) 307–318. doi:10.1007/s11745-013-3760-z.

[29] L.A. Carlson, Extraction of lipids from human whole serum and lipoproteins and from rat liver tissue with methylene chloride-methanol: a comparison with extraction with chloroform-methanol, Clin. Chim. Acta. 149 (1985) 89–93.

[30] J. Graessler, D. Schwudke, P.E.H. Schwarz, R. Herzog, A. Shevchenko, S.R. Bornstein, Top-Down Lipidomics Reveals Ether Lipid Deficiency in Blood Plasma of Hypertensive Patients, PLoS One. 4 (2009) e6261. doi:10.1371/journal.pone.0006261.

[31] V. Matyash, G. Liebisch, T. V Kurzchalia, A. Shevchenko, D. Schwudke, Lipid extraction by methyl-tert-butyl ether for high-throughput lipidomics, J. Lipid Res. 49 (2008) 1137–1146. doi:10.1194/jlr.D700041-JLR200.

[32] T. Pluskal, S. Castillo, A. Villar-Briones, M. Orešič, MZmine 2: Modular framework for processing, visualizing, and analyzing mass spectrometry-based molecular profile data, BMC Bioinformatics. 11 (2010) 395. doi:10.1186/1471-2105-11-395.

[33] M. Lísa, M. Holčapek, High-Throughput and Comprehensive Lipidomic Analysis Using Ultrahigh-Performance Supercritical Fluid Chromatography–Mass Spectrometry, Anal. Chem. 87 (2015) 7187–7195. doi:10.1021/acs.analchem.5b01054.

[34] S. Al Hamimi, M. Sandahl, M. Armeni, C. Turner, P. Spégel, Screening of stationary phase selectivities for global lipid profiling by ultrahigh performance supercritical fluid chromatography, J. Chromatogr. A. 1548 (2018) 76–82. doi:https://doi.org/10.1016/j.chroma.2018.03.024.

[35] N. Acar, O. Berdeaux, S. Grégoire, S. Cabaret, L. Martine, P. Gain, G. Thuret, C.P. Creuzot-Garcher, A.M. Bron, L. Bretillon, Lipid Composition of the Human Eye: Are Red Blood Cells a Good Mirror of Retinal and Optic Nerve Fatty Acids?, PLoS One. 7 (2012) 1–18. doi:10.1371/journal.pone.0035102.

[36] T.A. Lydic, G.E. Reid, W.J. Esselman, J. V Busik, Mass Spectrometry-Based Lipidomic Analysis of Rat and Human Retina, Invest. Ophthalmol. Vis. Sci. 48 (2007) 3068. http://dx.doi.org/.

[37] K.A. Zemski Berry, W.C. Gordon, R.C. Murphy, N.G. Bazan, Spatial organization of lipids in the human retina and optic nerve by MALDI imaging mass spectrometry, J. Lipid Res. . 55 (2014) 504–515. doi:10.1194/jlr.M044990.

[38] R. Mengual, Y. Segovia, M. García, Morphological Characteristics of Pilot Whales Retina (Globicephala melas; Traill, 1809) and their Relationship to Habitat, Int. J. Morphol. 32 (2014) 1399–1406.

[39] T.M. Attard, A.J. Hunt, Chapter 3. Supercritical carbon dioxide extraction of lipophilic molecules, in: A.J. Hunt, T.M. Attard (Eds.), Supercrit. Other High-Pressure Solvent Syst. Extr. React. Mater. Process., The Royal Society of Chemistry, London, 2018: pp. 30–75.

[40] N.E. Durling, O.J. Catchpole, S.J. Tallon, J.B. Grey, Measurement and modelling of the ternary phase equilibria for high pressure carbon dioxide-ethanol-water mixtures, Fluid Phase Equilib. 252 (2007) 103–113. doi:10.1016/j.fluid.2006.12.014.

[41] L.P. Cunico, C. Turner, Chapter 7 Supercritical Fluids and Gas-Expanded Liquids, in: 2019: pp. 155–214. doi:10.1016/b978-0-12-805297-6.00007-3.

[42] A. Forootan, R. Sjöback, J. Björkman, B. Sjögreen, L. Linz, M. Kubista, Methods to determine limit of detection and limit of quantification in quantitative real-time PCR (qPCR), Biomol. Detect. Quantif. 12 (2017) 1–6. doi:https://doi.org/10.1016/j.bdq.2017.04.001.

[43] P. Panuwet, R.E. Hunter Jr, P.E. D'Souza, X. Chen, S.A. Radford, J.R. Cohen, M.E. Marder, K. Kartavenka, P.B. Ryan, D.B. Barr, Biological Matrix Effects in Quantitative Tandem Mass Spectrometry-Based Analytical Methods: Advancing Biomonitoring, Crit. Rev. Anal. Chem. 46 (2016) 93–105. doi:10.1080/10408347.2014.980775.

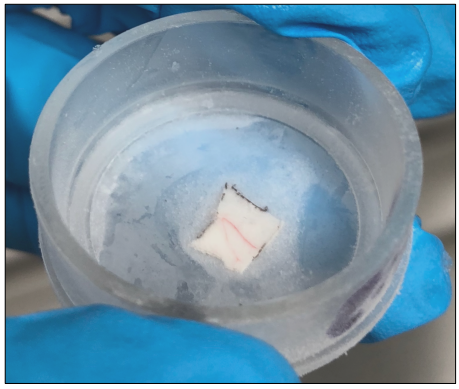

Figure S1. Section of retina tissue mounted in polycarbonate membrane (30 mm ⌀). Red lines correspond to veins in retina tissue.

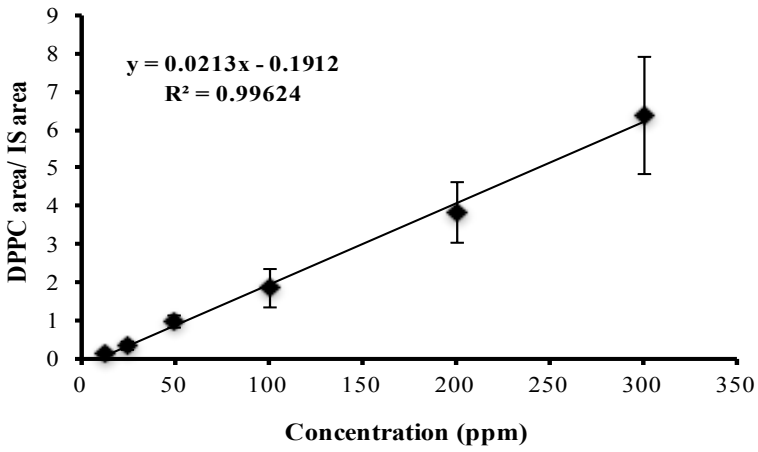

Figure S2. Calibration curve calculated from three independent curves using DPPC as standard and 15:0-18:1-d7-PC as internal standard (IS).

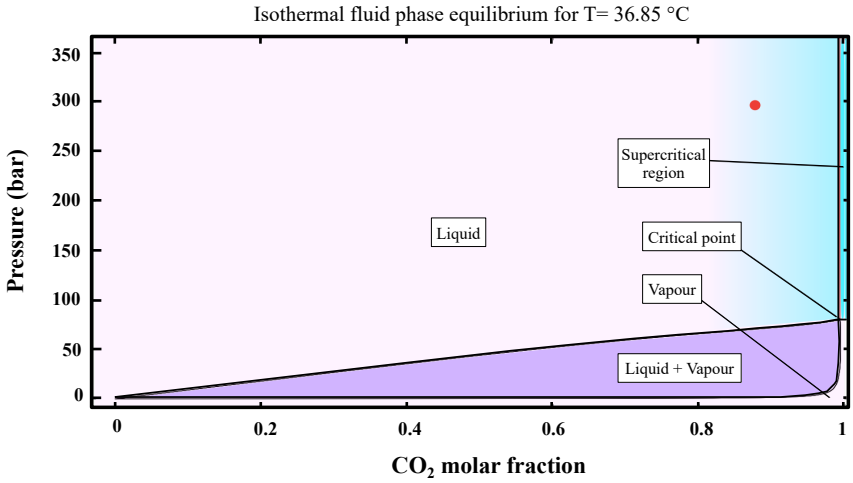

Figure S3. Binary pressure-composition phase diagram (GPEC 3.2.1, Phasety) for the CO_2-EtOH mixture at ~37°C. Red circle, localization of the used fluid in the phase diagram.

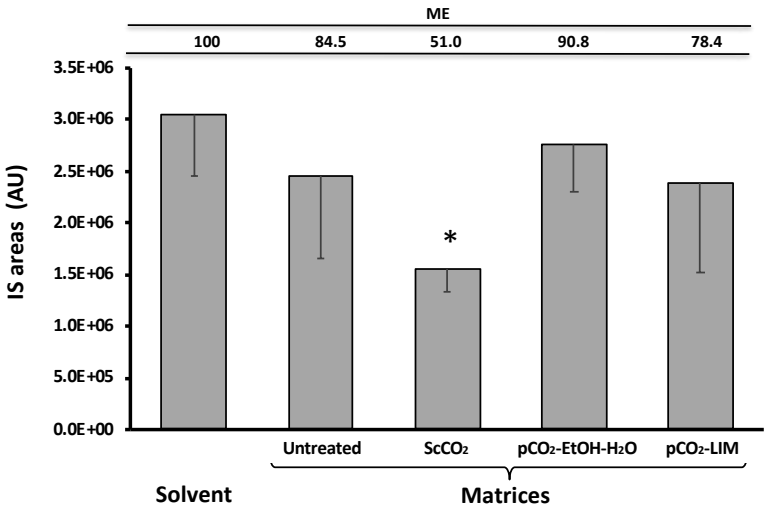

Figure S4. Representation of the matrix effect (ME) of respective matrices; untreated, pressurized (p)CO_2-limonene and neat scCO_2. MEs values are detailed on top of the bars, being 100% the IS signal in the solvent. *Data statistically different compared to the data from solvent (ANOVA, $p<0.01$). n=3 for untreated and scCO_2, n=1 for limonene. For solvent samples, it was considered the IS area of each point (six) per calibration curve (three).

Table S1. Signal-to-noise ratios (S/Ns) of the lipid species from untreated (A and C) and treated (B and D) samples. The possible effect of the treatment was approached by the untreated vs treated samples ratio, it is A/B and C/D ratios. *Ratios near to the unit, suggested no delipidation exerted by neat $scCO_2$ or pressurized CO_2-limonene fluids and, consequently, values >1 would indicate successful results.

Lipid specie	Untreated s4:3 S/N (A)	Neat $scCO_2$ treated s4:4 S/N (B)	A/B ratio*	Untreated s2:8 S/N (C)	Pressurized CO_2-limonene treated s2:7 S/N (D)	C/D ratio*
PC O-32:0	473.5	817.6	0.6	124.9	101.4	1.2
PC O-34:1; PC P36:1	1990.8	1972.7	1.0	642.1	589.7	1.1
PC 34:0	2713.8	2603.8	1.0	1125.6	769.6	1.5
PC 32:0	9500.9	9217.1	1.0	3846.3	3517.8	1.1
PC 32:1	132.0	152.7	0.9	32.0	23.1	1.4
PC 36:2	2956.0	3790.1	0.8	943.8	705.4	1.3
PC 34:1	872.9	825.8	1.1	401.5	324.7	1.2
PC 36:1	1839.9	2010.5	0.9	717.6	565.7	1.3
PC 36:3	6037.6	5436.4	1.1	2438.3	2526.6	1.0
PC 40:4	1775.5	2793.2	0.6	492.3	538.7	0.9
PC 38:4	13.9	19.4	0.7	3.3	0.1	27.9
PC 36:4	11.3	11.7	1.0	4.5	0.7	6.6
PC 38:6	35.1	32.2	1.1	7.1	2.2	3.3
PC 40:6	1125.8	1329.2	0.8	393.9	225.9	1.7
PC 38:7	9480.1	11453.5	0.8	3205.7	2648.4	1.2
PC 40:8	1380.3	1524.2	0.9	551.7	245.3	2.2
PE 36:1	498.5	545.2	0.9	155.0	59.2	2.6
PE O-34:2; PE P-34:1	315.7	284.6	1.1	87.3	59.4	1.5
PE 38:4	540.0	503.9	1.1	137.3	96.1	1.4
PE 40:4	66.8	44.3	1.5	14.3	10.4	1.4
PE O-38:6; PE P-38:5	113.2	137.0	0.8	38.8	12.0	3.2
PE O-40:7; PE P-40:6	2024.1	2051.2	1.0	570.8	404.7	1.4
PE 36:4	157.2	120.3	1.3	25.3	16.3	1.6
PE 40:6	6.7	6.3	1.1	2.9	0.4	7.8
PE 38:6	283.8	226.0	1.3	52.4	49.9	1.1
SM 40:1	1616.1	1950.2	0.8	301.8	250.3	1.2
SM 38:1	59.2	85.7	0.7	9.3	6.7	1.4
SM 36:1	1581.7	1573.3	1.0	316.0	262.9	1.2